## Title
Biosynthesis of Linear Protein Nanoarrays Using the Flagellar Axoneme



## Journal
ACS Synthetic Biology, 11(4)

## ISSN
2161-5063

## Authors
Ishikawa, Hiroaki
Tian, Jie L
Yu, Jefer E
et al.

## Publication Date
2022-04-15

## DOI
10.1021/acssynbio.1c00439

Peer reviewed

HHS Public Access

Author manuscript

*ACS Synth Biol*. Author manuscript; available in PMC 2022 December 15.

Published in final edited form as:

*ACS Synth Biol*. 2022 April 15; 11(4): 1454–1465. doi:10.1021/acssynbio.1c00439.

# Biosynthesis of linear protein nanoarrays using the flagellar axoneme

**Hiroaki Ishikawa**[1,2,#], **Jie L. Tian**[3,#], **Jefer E. Yu**[3], **Wallace F. Marshall**[1,2,*], **Hongmin Qin**[4,*]

[1]Department of Biochemistry & Biophysics, University of California San Francisco, San Francisco, CA 94143

[2]NSF Center for Cellular Construction, San Francisco, CA 94143

[3]Molecular & Environmental Plant sciences, Texas A&M University, College Station, TX 77845

[4]Department of Biology, Texas A&M University, College Station, TX 77845

## Abstract

Applications in biotechnology and synthetic biology often make use of soluble proteins, but there are many potential advantages to anchoring enzymes to a stable substrate, including stability and the possibility for substrate channeling. To avoid the necessity of protein purification and chemical immobilization, there has been growing interest in bio-assembly of protein-containing nanoparticles, exploiting the self-assembly of viral capsid proteins or other proteins that form polyhedral structures. But these nanoparticle are limited in size which constrains the packaging and the accessibility of the proteins. The axoneme, the insoluble protein core of the eukaryotic flagellum or cilium, is a highly ordered protein structure that can be several microns in length, orders of magnitude larger than other types of nanoparticles. We show that when proteins of interest are fused to specific axonemal proteins and expressed in living *Chlamydomonas reinhardtii* cells, they become incorporated into linear arrays which have the advantages of high protein loading capacity and single-step purification with retention of biomass. The arrays can be isolated as membrane enclosed vesicle or as exposed protein arrays. The approach is demonstrated for both a fluorescent protein (GFP) and an enzyme (beta-lactamase), showing that incorporation into axonemes retains protein function in a stable, easily isolated array form.

[*]Corresponding Author: Hongmin Qin, hqin@bio.tamu.edu; Wallace Marshall, wallace.marshall@ucsf.edu.
[#]Co-first-Author

Author Contributions

H.Q conceived the idea of axonemal protein nanoarrays and designed the overall project. H.I, J.L.T, and J.E.Y performed the experiments. W.F.M. analyzed data and wrote the initial draft of the manuscript, and all authors edited and revised the manuscript.

Supporting Information.

The supporting information associated with this paper consists of a Coomassie stained gel used to estimate flagellar protein quantity relative to a BSA standard (Supplemental Figure S1), an example plot showing the raw data from the nitrocefin beta lactamase assay (Supplemental Figure S2), a table of strains and plasmids used in this study (Supplemental Table S1), and five video images showing the motility phenotypes of mutant strains and the same mutant strains rescued with fusion protein constructs. These five videos are as follows: (Supplemental Movie S1) wild strain CC-125 demonstrating full motility; (Supplemental Movie S2) *dmj1-1* mutant defective in FAP20, showing impaired motility; (Supplemental Movie S3) *dmj1-1* mutant rescued with FAP20-βLac, showing recovery of motility thus confirming incorporation of the fusion protein into the axonemes; (Supplemental Movie S4) *pf14* mutant defective lacking RSP3 protein; (Supplemental Movie S5) *pf14* mutant rescued by expression of RSP3-βLac.

The authors declare no competing financial interest.

**Keywords**

Nanoparticles; Nanoarrays; Bionanotechnology; Protein Expression System; Green Algae

## Introduction

We often contrast biological systems with manmade systems by viewing biological machines as having structures that are intrinsically dynamic, characterized by large fluctuations in interactions and structure, compared to manmade machines that are rigid and precisely organized. This difference creates challenges for engineering biological systems to perform defined functions. As a result, much of biotechnology has historically focused on solution-phase enzyme systems. When it becomes necessary to immobilize enzymes or assemble them into structured arrays, this is done by isolating the enzymes and then using various physical or chemical means to immobilize them on artificial surfaces or particles. In certain cases, however, biology is able to build highly sophisticated and complex assemblies. Drexler has proposed that the ability of biomolecules to assemble into precisely organized solid-phase structures could be leveraged for synthetic biology purposes [1]. One of the most extreme examples of a complex molecular assembly is the eukaryotic flagellar axoneme, a linear structure in which hundreds of different proteins are docked in precise positions and defined orientations. We propose that the highly organized and regularly arranged structure of the axoneme can be engineered to allow stoichiometric production of protein components as immobilized linear nanoarrays. This approach confers several advantages, such as high protein loading capacity compared to other bioparticle systems; genetically programmed self-assembly without the need for any crosslinking steps; single-step purification of particles without the need for cell lysis, allowing retention and re-use of biomass; and choice of isolating the particle as a membrane enclosed vesicle or as an exposed protein array. This work will serve as the foundation for a new strategy for solid-phase synthetic biology that harnesses the precise assembly of cytoskeletal structures.

One straightforward application of solid-phase synthetic biology is in biocatalyst enzyme production, a core methodology in biotechnology. With the desire for increased protein production, multiple biotechnological methods have been developed. Enzymes are typically expressed in bacteria [2], yeast [3], insects, or mammalian cells [4] using recombinant molecular approaches. Optimizing these systems can require substantial effort to solubilize and purify the enzyme of interest. Moreover, even after enzymes are successfully produced and purified, they are easily degraded or inactivated, and difficult to store. Enzyme immobilization is an effective strategy to maximize both the physical and the enzymatic stability of a biocatalyst [5].

Immobilization strategies have evolved from simple physical absorption or covalent crosslinking onto insoluble carriers, such as agarose and Sepharose beads, or polypropylene, to the current focus on encapsulating enzymes into nanoparticles [6–8]. Encapsulation can provide stability and protection from the environment. The local concentration of protein within a particle can be extremely high, potentially allowing channeling of reaction products if enzymes responsible for sequential steps are included together in the same particle. This

channeling can lead to more efficient overall reactions as well as restricting the release of potentially toxic intermediates [9,10]. These desirable traits for medicine, research, and biotechnology have provided the impetus to search for systems and engineering approaches suitable for protein encapsulation. However, a major challenge remains how to incorporate a purified enzyme into a nanoparticle, via crosslinking or other strategies for attachment.

Naturally occurring self-assembled protein nanoparticles are excellent candidates for engineering protein encapsulates. For example, the carboxysome responsible for carbon fixation in some bacteria [11] and the polyketide synthase particle [12] can be harnessed to build synthetic nanoparticles containing a virtually limitless range of possible enzymes or other proteins of value. Nanoreactors based on bacteriophage MS2 capsid proteins [9] and the non-viral lumazine synthase protein [6] have been experimentally tested for their ability to encapsulate fixed quantities of enzymes. Using several different self-assembling protein scaffolds, it has been possible to build flexible engineering platforms to associate proteins into defined complexes, with demonstrable effects on metabolic flux [13–17]. Many of these proteins assemble into polyhedral shapes of defined size, creating a capsule with a lumen into which suitably tagged enzymes can be docked during particle assembly via protein-protein interactions. One limitation is the quantity of protein that can be incorporated. This is because the polyhedral geometry of the particle imposes a strict size limitation. Another limitation of these tightly packaged protein aggregates is that the enzyme's activity could be adversely affected due to misfolding or trapping toxic substrates [6].

Linear protein arrays present one possible alternative structure in which the size, and therefore the quantity of protein incorporated, could be much greater than in smaller polyhedral particles. There are many examples of proteins that self-organize into linear arrays within the cell. Examples include cytoskeletal filaments such as actin and tubulin as well as enzyme filaments such as glutamate synthase, CTP synthase, and the eIF2/2B complex [18,19]. While self-assembling filaments offer a way to increase protein content compared to polyhedral particles, they suffer from a much higher variability in total quantity. A population of self-assembling linear polymers is predicted to show an exponential distribution of lengths [20]. For certain applications, such as biosensors, where the total output of the array is to be measured, such a wide length distribution might be an unwelcome source of variability in output.

Inside of cells, cytoskeletal polymers show similarly wide length distribution making them non-ideal as protein carrier nanoarrays unless some method can be used to constrain length variation. The naturally occurring self-assembled protein nanoparticles and linear systems that have been adapted for engineering protein encapsulates are limited to particles with a diameter of 10 to 150 nm. Currently, no protein expression platform in use is capable of directly self-assembling protein arrays with defined size in living cells on a large size scale such as microns.

The flagellar axoneme of the green alga *Chlamydomonas reinhardtii* presents an ideal scaffold for constructing linear protein nanoarrays (Figure 1). The eukaryotic flagellum is a motile structure that consists of a protrusion of the plasma membrane supported by the axoneme, a protein-based assembly consisting of nine doublet microtubules (DMTs)

together with several hundred associated proteins involved in building the axoneme and driving flagellar motility. Flagellar proteins are synthesized in the cell body first and then make their way to the flagellum. A complex molecular machinery known as the intraflagellar transport (IFT) system uses a combination of motors and protein chaperones to transport insoluble proteins into the axoneme and incorporate them into the appropriate positions [21–23]. Many different proteins incorporate into the axoneme with fixed spatial repeats, for example, radial spokes and dynein arms bind to the axoneme with an underlying 96 nm periodicity that is generated by molecular rulers aligned to the axonemal lattice[24]. The *Chlamydomonas* axoneme therefore provides an excellent platform for the self-assembly of proteins on DMTs with high density and precise periodicity (Figure 1A).

In contrast to small sized polyhedral shape nanoparticles, axonemes typically are several orders of magnitude larger, on the 1-10 micron length scale. But unlike other large linear arrays such as microtubules or actin filaments, axonemes are subject to narrow length variation, typically showing a sharper-than-Gaussian [25] length distribution. Importantly, the length of the axoneme can be tuned using a collection of existing mutations [26], including mutants that have flagella that are longer than normal [27–29], and other mutants that have shorter flagella [30,31]. Length can also be tuned using chemical inhibitors. For example, lithium causes flagella to increase length [32], while other compounds obtained in chemical screens cause flagella to shorten [33,34]. Flagellar length is thus tunable via both genetic and chemical means.

Compared to other types of biological nanoparticles, axonemes are extremely easy to purify (Figure 1B). Flagella can be detached from living cells with a simple pH drop and purified with a single centrifugation step [35]. The cell bodies remain intact and viable, allowing for virtually complete recovery of biomass for further rounds of protein array production. The axoneme can then be obtained by treating the purified flagella with detergent, or else the whole flagellum can be used as a membrane-encapsulated array. Moreover, isolated flagella are stable and easily stored because no protease exists in the flagellar compartment [36].

As a source of biological material, the unicellular green alga *Chlamydomonas reinhardtii*, a genetically tractable green alga, can be grown at industrial scale using inexpensive media [26], and has been considered as a potential organism for production of algal biofuel. It can be cultured in large quantities with or without light. Other features that make this organism particularly useful include that it is safe for human consumption, and flagella can be repeatedly regenerated and isolated. Upon removal of its flagella, *Chlamydomonas* will regrow the structure within two hours [37], thus promoting rapid synthesis of desired protein products in a uniform array. Here we describe the use of the flagellar axoneme from *Chlamydomonas reinhardtii* as a platform for synthesis of self-assembled protein arrays in living cells.

## Results and Discussion

### Evaluating axonemal proteins as suitable adaptor for enzymes

The axoneme is a complex structure containing hundreds of different proteins [36]. In principle any of these could be used as an adaptor by fusing a protein domain of interest,

such as an enzyme, onto one end of the axonemal protein (Figure 1A). Then the adaptor fusion construct could be expressed in mutant cells that lack the endogenous copy of the adaptor protein encoding gene

As proof of concept, we examined three candidate adaptor proteins: IFT20, RSP3, and FAP20 (Figure 2). IFT20 is a protein subunit of IFT particles [38]. RSP3 is part of the radial spoke complex, a T-shaped complex that is composed of at least 23 proteins [39]. The radial spoke stalk is anchored to the inner side of doublet microtubules and its globular head extends toward the central pair of singlet microtubules. In each 96 nm periodic structure, there are two complete radial spokes and one truncated spoke [40]. RSP3 is encoded by the *PF14* gene, and *pf14* loss-of-function mutants have paralyzed flagella [41]. FAP20 is a component of the inner junction (IJ) filament complex, a protein complex located at the seam between the A and B tubules of the outer doublet microtubules [42]. FAP20 lines the IJ of the doublet microtubule at a precise 8 nm periodicity, forming 9 parallel solid nanoarrays [43]. The relative locations of these three adaptor proteins are shown in Figure 2A.

To evaluate adaptor proteins, we expressed GFP-tagged versions of these three candidate adaptor proteins in *Chlamydomonas* cells under control of endogenous promotors. GFP fusions of IFT20 [44], RSP3 [45], and FAP20 [43] (Figure 2B) have all been previously described in the literature. Importantly, all three were shown to rescue loss of function mutations in the corresponding gene even when fused to GFP, indicating that the GFP fusion does not interfere with function. Visual comparison (Figure 2C) showed that FAP20-GFP showed the brightest signal, indicating the largest quantity of protein incorporated into the axoneme.

As a quantitative comparison for incorporation among the different scaffold proteins, we implemented an automated segmentation procedure for flagella, which traces the linear background of each flagellum, and quantifies fluorescence intensity as a function of position (Figure 3A). Segmentation of flagella was performed by first identifying the cell body, subtracting it from the image, and then traversing each flagellum, starting at the two tips and identifying neighboring pixels of maximal intensity. This method was able to reliably label each flagellum (Figure 3B) allowing GFP intensity to be quantified specifically inside the flagella, without interference from the cell body. Using this algorithm, we quantified the total fluorescence intensity in each of the three strains (Figure 3C). In all three cases, we found that the total intensity scales linearly with the flagellar length. For any particular length, FAP20-GFP always gave the highest total intensity, and RSP3 the lowest, suggesting that the FAP20 scaffold is more effective than the other two in terms of protein incorporation into the flagellum. Scatter of points around the best fit lines in Figure 3C indicated that IFT20 shows substantially greater variation than RSP3 which had a similar average intensity. This is perhaps to be expected, given that the IFT complexes localize sparsely along the flagellum and undergo constant transport in and out of the flagellar compartment [46]. This analysis demonstrates that for all constructs tested, incorporation is directly proportional to length, but that compared to IFT20 and RSP3, FAP20 shows the highest fluorescence per unit length, confirming that this fusion results in the highest level of functional GFP incorporation into the axoneme. We also noted visually in Figure 2 that FAP20 shows the most spatially uniform incorporation along the length of the flagellum. These results indicate that FAP20 may be the most suitable scaffold protein for building axonemal protein arrays.

As an estimate of the yield of FAP20 fusion obtained by this procedure, we note that standard flagellar isolations from *Chlamydomonas* produce a yield of 1 mg of flagellar protein per 1 L of culture of *Chlamydomonas* culture at 5 x $10^7$ cells/mL. Based on peptide count data from the Chlamydomonas flagellar proteome (http://chlamyfp.org) [36], FAP20 protein represents approximately 0.3% of axonemal protein. Thus, we estimate that the yield of FAP20 fusion from a 1 L culture will be roughly 3 μg.

## Stability of protein arrays during isolation and storage

Easy isolation and high stability during both isolation and storage are essential for any sort of nanoparticle or nanoarray to be useful in practice. *Chlamydomonas* cells sever flagella at the base when placed under stress conditions, for example pH shock [47]. The flagella can then be cleanly separated away from the cell bodies by centrifugation through a sucrose cushion [48]. These flagella can then be frozen down for storage or else demembranated to produce isolated axonemes (Figure 1B).

Axonemes are stable structures, but the degree to which individual axonemal proteins can remain stably anchored to axonemes has never been systematically addressed. We have found that FAP20-GFP is retained during isolation of flagella as well as following demembranation to produce axonemes (Figure 4). For both flagella and axonemes, FAP20-GFP was retained during freezing and thawing (Figure 4E). The high stability of protein arrays on flagellar axoneme during isolation and storage is desirable for practical usage.

## Using ß-Lactamase to evaluate biosynthesis of enzyme axonemal nanoarrays

As a proof of concept for enzyme incorporation into axonemal arrays, we expressed β-Lactamase (βLac) fused to FAP20 and RSP3 as adaptors to evaluate if flagellar axonemes are suitable for biosynthesis of enzyme nanoarrays. Because of the sparse localization of IFT20, we did not evaluate it as a scaffold in these experiments. βLac has been tested in self-encapsulation using lumazine synthase protein [6], in which it could be efficiently encapsulated, but the encapsulated enzyme showed more than a 10-fold drop in catalytic efficiency compared to soluble βLac. Protein misfolding was likely responsible for the reported loss of the catalytic activity, which is notoriously difficult to deal with. We expressed FAP20-TEV-βLac or RSP3-TEV-βLac constructs (Figure 5A), using integrated constructs under control of endogenous promotors for FAP20 or RSP3 respectively, in *Chlamydomonas* strains carrying the non-motile loss-of-function mutants *dmj1-1 (fap20)*[43] or *pf14 (rsp3)*[41], respectively. The cells expressing the fusion proteins became motile because of the expression of adaptor proteins and were identified by microscopic observation (Supplemental Movies S1–S5). The protein concentration of all flagella samples was quantified by comparing to BSA standard samples (Supplemental Figure S1). The concentration of each sample was adjusted to 1.6 μg/μL and then subjected to Western blotting. The expression of target protein βLac was immunoblotted by βLac antibody, and wild-type (WT) flagella samples were used as a negative control. In order to evaluate whether yield of flagellar protein could be maintained when flagella are removed and regenerated, FAP20-βLac flagella were regenerated once, and RSP3-βLac flagella were regenerated twice due to the shorter flagellar regeneration time. Immunoblotting of acetylated tubulin confirmed that all samples had equal loading of flagellar axonemes

(Figure 5B), confirming that the yield of FAP20 in each sample was maintained when flagella regenerate.

We measured the βLac catalytic activity using a colorimetric Beta Lactamase Activity Assay Kit (Supplemental Figure S2 see Methods) to compare the catalytic efficiency of FAP20-TEV-βLac or RSP3-TEV-βLac in the isolated flagella to commercial βLac enzyme. Wild-type *Chlamydomonas* cells do not possess measurable endogenous βLac activity (Figure 6A), but when either the FAP20 or RSP3 fusions with βLac were expressed, isolated flagella showed clear enzymatic activity that was proportional to the quantity of flagella tested (Figure 6A,B).

Our assays show detectable enzymatic activity that is not present in control flagella lacking the fusion proteins. The next question is how much of the enzyme present in the axonemes is functional. The FAP20-βLac or RSP3-βLac fusion proteins only represent a small fraction of the total flagellar protein. As discussed in Methods, we estimated how much of the loaded protein represents the enzyme fusion using two different approaches, one based on proteomic data and one based on the stoichiometry of FAP20 or RSP3 relative to tubulin based on electronic microscopy structural analyses. The two methods (proteome based or structure based) provide estimates for FAP20-fused βLac protein ranging from 0.0015 mg to 0.007 mg, per 1 mg of total flagellar protein. Likewise, the two methods yield estimates for RSP3-fused βLac ranging from 0.0006 mg to 0.003 mg per 1 mg of total protein.

Based on Figure 6A, 40 μg of flagella containing FAP20-βLac gave 25 mU of activity, giving a specific activity 0.625 U/mg of total flagellar protein. Converting to mg of FAP20/mg of total flagellar protein, using the range obtained from the proteomic and structure-based estimates (see Methods), we obtain a specific activity of FAP20-fused βLac in the range 90-400 U/mg. For the RSP3 fusion, 50 μg of flagella containing RSP3-βLac gave 17 mU of activity, which, converting to mg of RSP3/mg of total flagellar protein using our proteomic and structure-based estimates (see Methods), yields a specific activity of 110-560 U/mg of βLac fusion. The predicted specific activity for βLac in the context of the two fusion proteins is thus in the same range. Moreover, the range of estimated specific activity is comparable to the specific activity of purified TEM-1 βLac which has been reported to be 366 U/mg using the nitrocefin assay under identical conditions[49]. These results imply that fusion of the βLac enzyme to axonemal scaffold proteins does not significantly impair enzyme activity. Furthermore, the fixed enzymes on axonemes appeared resistant to freeze-thaw treatment, and stable for room temperature storage (Figure 6B). Protein arrays also retained enzymatic activity when separated from substrate and then used for a new round of assays (Figure 6C).

## Release of attached proteins by TEV protease cleavage

We envision the axonemal array system as a flexible platform for building structured arrays of immobilized proteins in fixed relative orientations. However, because the IFT system can handle insoluble proteins as part of its normal function, we propose that axonemal protein arrays might also be useful as protein expression systems. In this case, a method would be needed to release the protein from the rest of the axoneme. To test this idea, we generated a variant construct in which the FAP20 and GFP domains were linked by a linker containing a

TEV protease cleavage site (Figure 7A). Flagella were harvested from strains expressing this construct, and used to prepare axonemes. Experiments confirm that the vast majority of GFP was removed following TEV protease treatment of the isolated axonemes (Figure 7B).

## Design challenges for axonemal enzyme arrays

We have shown that the axoneme is a flexible platform for biological assembly of protein arrays, able to incorporate at least two structurally distinct protein clients (GFP and βLac) while retaining their function. Future work will be needed to determine the range of proteins that are compatible with this platform. The size, charge, and quaternary structure of target proteins may affect their ability to enter the flagellar compartment as well as to fit stably into the context of the axoneme. These constraints are not unique to axonemes - in other cases of biological nanoparticles, protein charge and size clearly affects the level of incorporation [6]. The evolutionary selection of the IFT system to transport extremely large protein complexes such as dynein arms and radial spokes suggests that axonemal assembly may be particularly amenable to a wide range of target proteins.

Given that an enzyme can be efficiently incorporated into an axonemal array, the next concern is to ensure that the enzyme will be active. Enzymes can be strongly affected by their chemical environment in terms of such parameters as pH and salt concentrations. We hypothesize that enzymes will experience unique chemical environments when incorporated into axonemal protein arrays, and will be most effective in these arrays if the enzyme is selected so that the chemical environment of the flagellum or axoneme is matched to the optimal conditions for catalysis by the enzyme. Microtubules are negatively charged, with a charge density on the microtubule surface of −2.5 e/nm along a protofilament [50]. FAP20 is located within 10 nm of this charged microtubule surface [43], well within the Debye length for sodium ions at physiological salt (70 nm)[51] and will, therefore, be within an appropriate distance to feel the altered ionic concentration. We therefore hypothesize that an enzyme docked on the axoneme using FAP20, will be surrounded by a different ionic environment than that of the bulk solution, even in isolated axonemes without a membrane. For enzymes docked using the RSP3 as a scaffold, the effect will be even larger since the radial spoke is buried within the interior of the axoneme. It is interesting to consider whether the distinct charged environments with an axoneme could be exploited.

## Towards solid-phase synthetic biology

Compared to physical immobilization of proteins on beads or other artificial substrates, the use of biologically self-assembling scaffolds should help to facilitate exploration of this type of approach for an increasing range of enzymes or other proteins, because different constructs can be readily tested just by transforming them into cells. In addition to the biological nanoparticles mentioned above, a recent modular system for assembling proteins into structures using bacterial nanocompartment proteins has been described that is specifically designed to facilitate attaching a wide range of target proteins into the assembled structure [52]. In that system, it was shown that incorporation into the assembly leads to increased protein stability and activity [52]. We believe that the axoneme may provide a large, easy to purify complement to these prokaryotic structure based approaches.

Although we have focused on the ability to isolate axonemal arrays for in vitro applications, it is also possible that the protein arrays might be used within a living cell, for example to compartmentalize reactions inside the flagellum whose products may be toxic in the cytoplasm. The use of self-assembled protein structures inside of bacterial cells has been reported using bacterial microcompartment proteins [53].

In addition to the potential advantages of protein arrays for enzyme applications discussed above, such as easy purification, reusability of biomass, and in vivo production of enzymes that might not be amenable to overexpression and isolation on their own, the ability to dock proteins of interest into spatially patterned arrays may open up a new strategy for implementing logic and computational processes using biological molecules. Much work in synthetic biology focuses on solution phase biochemistry. Examples include re-engineering gene regulatory networks in which soluble transcription factors bind and unbind from promoters [54] or re-wiring signaling networks mediated by reversible protein-protein interactions [55]. From a circuit design perspective, the fact that a given protein is free to diffuse throughout the cell means that one protein species can only carry one signal. If we want to add a second signal into the circuit, we need to add a second protein species. This creates a huge challenge for engineering any but the most trivial of circuits. In electronics, complex circuitry was made possible by the fact that each component is irreversibly locked into position, and the interactions between components are rigidly defined by the wires to which they are attached. By locking proteins into position on the axoneme or other insoluble cellular structures, we can limit their potential interactions to their nearest neighbors. How to exploit such spatially restricted interactions is still an open question, but we note that there are already paradigms in computer science and engineering in which an array of identical devices, that can only interact with their immediate neighbors, can carry out complex computational tasks. Specific examples include the large class of models known as “cellular automata” [56] as well as fixed networks of locally coupled oscillators [57,58].

## Concluding Remarks

We have shown that the flagellar axoneme provides a platform for bio-assembly of linear protein arrays. We find that different axonemal proteins can be used as scaffolds to attach other protein moieties as fusion constructs. Proteins linked to the axoneme in this way retain activity, but can be liberated from the axoneme using site specific proteases. The axoneme system is highly scalable at low cost given the biological self-assembly of immobilized arrays, the fact that algal cells can be grown without providing a carbon source in the media, and the ability to isolate the arrays using a one-step purification that retains biomass of the producing cell. The uniform, high packing density of axonemal proteins with precise relative protein orientations creates new potential opportunities for substrate channeling, biosensing, and protein-based computation.

## Methods

### Chlamydomonas culture and imaging

*Chlamydomonas* cultures were grown in Tris-acetate-phosphate (TAP) media (20 mM Tris HCl, 3.5 mM $NH_4Cl$, 0.2 mM $MgSO_4$, 0.17 mM $CaCl_2$, 1 mM $K_3PO_4$, and Hutner’s

trace elements (1:1000), titrated to pH 7.0 with glacial acetic acid) [59] at 25°C, with constant aeration and continuous light. For imaging fixed cells, *Chlamydomonas* cells were attached to polylysine-coated coverslips and then fixed with 4% paraformaldehyde in PBS for 5 min. Cells were then mounted in Vectashield (Vector Laboratories, Burlingame, CA) on a slide and imaged using a spinning disk confocal microscope (Eclipse Ti; Nikon, Tokyo, Japan) with a 100x oil objective (Apo TIRF, NA 1.49; Nikon), confocal system (CSU-22; Yokogawa Electric Corporation, Japan), and an EMCCD camera (Evolve Delta; Photometrics, Tucson, AZ). 3D images were taken with a z-axis spacing of 0.2 μm.

Flagellar length and fluorescent intensity were measured using custom-written routines in MATLAB (MathWorks, Natick, MA). Z-stack images were convolved with a three-dimensional Gaussian filter to detect the cell body position by finding the center of mass. The cell body was subtracted from the original z-stack images, such that the remaining intensity was restricted to the flagella, after which the position of flagellar tips was detected. Flagellar position was then identified by moving backwards from the flagellar tip step by step on the basis of the local intensity. The MATLAB code is available on Github (https://github.com/ishikawaUCSF/2022ACSSynBio).

## Preparation and storage of flagella and axonemes

Isolation of flagella was performed as described [48]. Briefly, Chlamydomonas were grown in TAP media until the culture turned dark green (5 x $10^7$ cells/mL). Flagella were released from the cell body using pH shock, by adding acetic acid to lower pH to 4.0, incubating for 1 min, and then returning to pH 7.0 using KOH [48]. Flagella were then separated from the cell bodies by centrifugation at 1,800 ×g for 5 min at 4°C. Supernatant was then transferred to the top of a 25% (v/v) sucrose cushion in a 50 mL conical tube and centrifuged at 2,400 ×g for 10 min at 4°C. To concentrate flagella, the supernatants were then pelleted at 30,000 ×g for 20 min at 4°C. The pellets were resuspended in HMDEK buffer (30 mM HEPES, pH 7.4, 5 mM $MgSO_4$, 1 mM DTT, 0.5 mM EGTA, and 25 mM KCl). To remove the membrane, we added 1% NP-40 (v/v) to the flagellar suspension and incubated it for 10 min on ice. The axonemes (demembranated flagella) were centrifuged at 30,000 ×g for 20 min at 4°C and resuspended in HMDEK buffer. Isolated flagella and axonemes were flash frozen in liquid nitrogen and stored at −80°C for 3 days. Fresh and frozen flagella were observed to quantify the GFP intensity using a spinning disk confocal microscope (Eclipse Ti; Nikon). The GFP intensity was quantified using a MATLAB script which can be downloaded from Github (https://github.com/ishikawaUCSF/2022ACSSynBio).

## TEV protease cleavage

Isolated axonemes were treated with TEV protease (GenScript, Piscataway, NJ) overnight at 4°C, then centrifuged at 20,000 ×g for 20 min to pellet the axonemes. The protease-treated axonemes were then attached to poly-L-lysine-coated coverslips, fixed with ice-cold methanol, blocked with 5% BSA, 1% fish gelatin, and 10% normal goat serum in PBS, and then incubated with mouse anti-GFP monoclonal antibody (1:1000; Roche, Indianapolis, IN) as well as rabbit anti-alpha-tubulin polyclonal antibody (1:1000; Abcam, Cambridge, United Kingdom). Following primary staining, axonemes were washed with PBS and incubated with mouse-Alexa488 and rabbit-Alexa546 antibodies (1:200; Invitrogen, Waltham, MA).

Samples were washed with PBS and mounted with Vectashield, then imaged using a DeltaVision microscope (GE Healthcare, Chicago, IL) equipped with a 100x oil objective (Olympus, Tokyo, Japan). Z-stacks were collected at an interval of 0.2 μm, then deconvolved and projected with DeltaVision software (GE Healthcare). For quantification of GFP release by TEV protease, we measured intensities of GFP and alpha-tubulin on projected images. The signal of alpha-tubulin was hand-traced with the segmented line tool with 11-pixel line width and measured average intensity of both GFP and alpha-tubulin using ImageJ (NIH).

## Fusion constructs

All constructs (Supplemental Table S1) were built based on the plasmids pBS-FAP20-C-ERV and pKF-RSP3-GFP, described in a previous publication [43]. Using these plasmids as a starting point, the rescue constructs were generated using a combination of gene synthesis and standard cloning methods by GenScript (Piscataway, NJ). Sequence optimization was performed by Serotiny (San Francisco, CA). The new constructs were assembled so as to substitute the *GFP* gene with the target protein gene in both pBS-FAP20-GFP and pKF-RSP3-GFP. In the new sequences, the *Eco*RV linker and *GFP* gene were deleted. In the pKF-RSP3-GFP construct, the C-terminal 140 amino acids of RSP3 were also deleted to generate more space for the target protein because the last 140 amino acids of RSP3 do not affect either recruitment of radial spoke proteins assembled on the axoneme or the motility of flagella [45]. Furthermore, the target protein genes following the TEV linker were inserted behind the adaptor protein gene. In this case, Serotiny first made the vectors pBS-FAP20-TEV-X and pKF-RSP3-TEV-X, and then inserted Beta-lactamase or GFP gene into the vector using the restriction enzyme sites *Nde*I and *Xho*I. The Beta lactamase sequenced was a Chlamydomonas codon-optimized version of TEM-1 beta lactamase.

## Rescue of dmj1-1 and pf14

The plasmid FAP20-TEV-βLac was used to rescue the *dmj1-1* strain. The plasmid RSP3-TEV-βLac was used to rescue the *pf14* strain. Both plasmids were linearized with *Ssp*I enzyme, linearized FAP20-TEV-βLac are transformed together with the paromomycin-resistant pSI103 plasmid for selection. Plasmid RSP3-TEV-βLac carries the paromomycin-resistant gene itself. The electroporation technique was applied to transform *Chlamydomonas* cells. Briefly, *dmj1-1* or *pf14* cells were cultured in 100 mL TAP medium to dark green, then transferred to 1 L TAP medium with constant aeration. The cells are ready to be transformed when the concentration reaches $10^6$ cells/mL about 20 hours later. In total, $10^8$ cells were collected and resuspended in 1 mL TAP liquid media containing 60 mM sorbitol. 300 μL of cell suspension was transferred to a 4-mm electroporation cuvette. For the *dmj1-1* cells, 600 ng linearized FAP20-TEV-βLac together with 300 ng pSI103 plasmids were added and mixed evenly. For the *pf14* cells, 600 ng linearized RSP3-TEV-βLac plasmids were used instead. The mixture of plasmids and cells in the cuvettes were chilled on ice for 5 min and then electroporated with an ECM630 electroporator (BTX, Holliston, MA) with the setup parameters of capacitance 50 μF, resistance 650 Ω, and the voltage 825 V. The cells were allowed to recover on ice for 15 min after electroporation and then transferred to 10 mL TAP medium with 60 mM sorbitol and cultured for 24 hours in a low light environment. The next day, cells were collected and plated on TAP plates containing 10 ng/μL paromomycin to grow 4-5 days to obtain transformants. We note that

in *Chlamydomonas*, transformed plasmids integrate into the genome at random and are not maintained as free plasmids.

### Prescreening rescue colonies by observing cell motility and flagellar assembly

After spreading transformed cells on TAP plates containing paromomycin for 4-5 days, we transferred resistant colonies to 96 well plates with liquid TAP medium. Cell motility was observed under an inverted microscope (CKX53, Olympus) after 24 hours of culture. Colonies containing motile cells were further cultured in 3 mL TAP medium for two days, after which cell motility and flagellar length were observed with an Axioplan phase contrast microscope (Carl Zeiss, Oberkochen, Germany) with a 4x objective.

### Flagella regeneration

The protocol for flagella regeneration is modified slightly from that used in the flagella isolation method. Instead of underlaying the sample with 25% sucrose immediately after pH shock, the flagella and cell bodies were separated by centrifuging at 2,000 rpm, 5 min, 18°C. The supernatant contains the flagella and was subjected to the 25% sucrose underlay to collect flagella, while the cell bodies were resuspended in 500 mL HEPES to culture 1-2 hours to regenerate flagella.

### Flagella enzymatic activity assay under different treatments

Soluble βLac enzyme provided in the enzyme assay kit (abcam ab197008), isolated FAP20-βLac, or RSP3-βLac flagella were either used freshly, freeze-thawed 4 times between −20 and 20°C, treated 10 min at 42°C, or kept at room temperature for 48 hours (overnight) depending on the experiment and as indicated in the graphs. 2.5 μg of commercial soluble βLac enzyme, and 8 μg flagellar samples were subjected to beta-lactamase activity assay. Untreated fresh flagella or soluble commercial protein were used as controls. Once the commercial βLac enzyme or flagella samples were mixed with nitrocefin to start the reactions, the absorbance at 490 nm for each sample was measured every minute until the absorbance reached a plateau. The concentration of the products was calculated based on the standard formula $y = 0.0185x + 0.0318$ (Supplemental Figure S2). The enzymatic activity was calculated at 1 min, 2 min, and 3 min. The enzymatic activity was calculated by averaging three measurements with standard deviation. βLac activity was expressed as μmoles/min hydrolyzed nitrocefin generated per mg of protein (U/mg). In our experiments, 2.5 μg of commercial enzyme gave 12.7 mU of activity as defined with the nitrocefin assay. This corresponds to a specific activity of 5 U/mg.

### Estimating quantity of fusion proteins in flagellar preparations

We used two approaches for estimating the fusion protein quantity in the flagella samples used for enzymatic assays. The first approach takes advantage of proteomic analyses of isolated *Chlamydomonas* flagella and axonemes, in which we can estimate the fraction of flagellar protein represented by FAP20 or RSP3 by dividing the number of peptide hits for each of these proteins with the total number of peptide hits detected in the entire analysis. Using data from three different proteomic analyses [36,60,61] this calculation indicates that Fap20 constitutes 0.3%, 0.1%, and 0.2% respectively for the three different proteomic

datasets. A similar calculation indicates that according to the three studies, RSP3 constitutes 1%, 0.2%, and 0.5% of the total protein, respectively. We can then estimate the total quantity of βLac in the flagellar samples by multiplying the quantity of sample loaded by the fraction of total protein, and then multiplying this by the ratio of molecular weights of FAP20 (20 kDa), RSP3 (96 kDa) and βLac (29 kDa). Using the range of values between 0.1% to 0.3%, this calculation indicates that 1mg of total flagellar protein will contain from 0.0015 to 0.007 mg of βLac fused to FAP20. A similar calculation for RSP3 (96 kDa) indicates that 1 mg of total flagellar protein should contain from 0.0006 to 0.003 mg of βLac fused to RSP3.

Our second approach for estimating protein quantity is to take advantage of structural knowledge. Structural studies of the axoneme [42,43,62,63] show a 96 nm repetitive structure. FAP20 repeats every 8 nm along each of 9 doublet microtubules, giving 108 molecules of FAP20 per 96nm repeat. α, β-tubulin dimers are 8 nm long and compose 9 doublet microtubules, each containing 23 protofilaments plus a central pair of singlet microtubules which jointly contain 26 protofilaments. The number of α, β-tubulin dimers per 96nm repeat is thus 2796. The molar ratio of FAP20 to tubulin dimers is thus 0.04. Biochemical estimates have found that approximately 40% of the protein mass of *Chlamydomonas* axonemes is tubulin[64], such that 1 mg of flagella would contain roughly 0.4 mg of tubulin. Combining the molar ratio of FAP20 to tubulin with the relative molecular weight of βLac versus the tubulin dimer, we estimate that 1 mg of flagella will contain (0.4mg/100kDa tubulin) * 0.04 * 29kDa = 0.0045 mg βLac fusion. Note that for purposes of comparing estimated specific activity of βLac in the fusion form to βLac in published assays, we calculate the quantity of βLac protein itself even though this protein is fused to other proteins. RSP3 is part of the radial spoke complex, which is a dimer that repeats on average 2.5 times per 96 nm of the axoneme, along each of the nine outer doublets, yielding 45 RSP3 molecules per 96 nm. The molar ratio of RSP3 to tubulin is thus 0.016. We therefore estimate that 1mg of flagella will contain (0.4/100kDa)*0.016*29kDa = 0.002 mg of βLac.

## Supplementary Material

Refer to Web version on PubMed Central for supplementary material.

## Acknowledgments

We thank members of the Marshall and Qin laboratories for helpful discussion. This work was supported by TAMU T3 grant 02246495 and STRP 290166 (H.Q), NIH grant R35 GM130327 (W.F. M.) and by the Center for Cellular Construction, an NSF-funded Science and Technology Center supported by NSF grant DBI1548297 (W.F.M.)

## References

1. Drexler KE (1992) Nanosystems: Molecular Machinery, Manufacturing, and Computation. Wiley. 576 pp.
2. Rosano GL, Morales ES, and Ceccarelli EA (2019) New tools for recombinant protein production in Escherichia coli: A 5-year update. Protein Sci. 28, 1412–1422. [PubMed: 31219641]
3. Baghban R, Farajnia S, Rajabibazl M, Ghasemi Y, Mafi A, Hoseinpoor R, Rahbarnia L, and Aria M (2019) Yeast Expression Systems: Overview and Recent Advances. Mol Biotechnol. 61, 365–384. [PubMed: 30805909]
4. McKenzie EA, and Abbott WM (2018) Expression of recombinant proteins in insect and mammalian cells. Methods. 147, 40–49. [PubMed: 29778647]

5. Basso A, and Serban S (2019) Industrial applications of immobilized enzymes-A review. Mol Catal. 479, 35–54.
6. Azuma Y, Zschoche R, Tinzl M, and Hilvert D (2016) Quantitative Packaging of Active Enzymes into a Protein Cage. Angew Chem Int Ed Engl. 55, 1531–1534. [PubMed: 26695342]
7. Datta S, Christena LR, and Rajaram YRS (2013) Enzyme immobilization: an overview on techniques and support materials. Biotech. 3, 1–9.
8. Plegaria JS, and Kerfeld CA (2018) Engineering nanoreactors using bacterial microcompartment architectures. Curr Opin Biotechnol. 51, 1–7. [PubMed: 29035760]
9. Giessen TW, and Silver PA (2016) A Catalytic Nanoreactor Based on in Vivo Encapsulation of Multiple Enzymes in an Engineered Protein Nanocompartment. Chembiochem. 17, 1931–1935. [PubMed: 27504846]
10. Khattak WA, Ullah MW, Ul-Islam M, Khan S, Kim M, Kim Y, and Park JK (2014) Developmental strategies and regulation of cell-free enzyme system for ethanol production: a molecular prospective. Appl Microbiol Biotechnol. 98, 9561–9578. [PubMed: 25359472]
11. Rae BD, Long BM, Badger MR, and Price GD (2013) Functions, compositions, and evolution of the two types of carboxysomes: polyhedral microcompartments that facilitate CO2 fixation in cyanobacteria and some proteobacteria. Microbiol Mol Biol Rev. 77, 357–379. [PubMed: 24006469]
12. Fischbach MA, and Walsh CT (2006) Assembly-line enzymology for polyketide and nonribosomal Peptide antibiotics: logic, machinery, and mechanisms. Chem Rev. 106, 3468–3496. [PubMed: 16895337]
13. Dueber JE, Wu GC, Malmirchegini GR, Moon TS, Petzold CJ, Ullal AV, Praher KLJ, and Keasling JD (2009) Synthetic protein scaffolds provide modular control over metabolic flux. Nat. Biotechnol 27, 753–9. [PubMed: 19648908]
14. Price JB, Chen L, Whitaker WB, Papoutsakis E, and Chen W (2016) Scaffoldless engineered enzyme assembly for enhanced methanol utilization. Proc. Natl. Acad. Sci. U.S.A 133, 12691–12696.
15. Heater BS, Lee MM, and Chan MK (2018) Direct production of a genetically-encoded immobilized biodiesel catalyst. Sci. Rep 8, 12783. [PubMed: 30143735]
16. Nichols TM, Kennedy NW, and Tullman-Ercek D (2019) Cargo encapsulation in bacterial microcompartments: methods and analysis. Meth. Enzymol 617, 155–186.
17. McConnell SA, Cannon KA, Morgan C, McAllister R, Amer BR, Clubb RT, and Yeates TO 2020. Designed protein cages as scaffolds for building multienzyme materials. ACS Synth. Biol 9, 381–391. [PubMed: 31922719]
18. Noree C, Sato BK, Broyer RM, and Wilhelm JE (2010) Identification of novel filament-forming proteins in Saccharomyces cerevisiae and Drosophila melanogaster. J Cell Biol. 190, 541–551. [PubMed: 20713603]
19. Ingerson-Mahar M, Briegel A, Werner JN, Jensen GJ, and Gitai Z (2010) The metabolic enzyme CTP synthase forms cytoskeletal filaments. Nat. Cell Biol 12, 739–46. [PubMed: 20639870]
20. Oosawa F, and Kasai M (1962) A theory of linear and helical aggregations of macromolecules. J Mol Biol. 4, 10–21. [PubMed: 14482095]
21. Ishikawa H, and Marshall WF (2011) Ciliogenesis: building the cell's antenna. Nat Rev Mol Cell Biol. 12, 222–234. [PubMed: 21427764]
22. Qin H (2012) Regulation of intraflagellar transport and ciliogenesis by small G proteins. Int Rev Cell Mol Biol. 293, 149–168. [PubMed: 22251561]
23. Qin HM, Diener DR, Geimer S, Cole DG, and Rosenbaum JL (2004) Intraflagellar transport (IFT) cargo: IFT transports flagellar precursors to the tip and turnover products to the cell body. Journal of Cell Biology. 164, 255–266. [PubMed: 14718520]
24. Oda T, Yanagisawa H, Kamiya R, and Kikkawa M (2014) A molecular ruler determines the repeat length in eukaryotic cilia and flagella. Science. 346, 857–860. [PubMed: 25395538]
25. Kannegaard E, Rego EH, Schuck S, Feldman JL, and Marshall WF (2014) Quantitative analysis and modeling of katanin function in flagellar length control. Mol Biol Cell. 25, 3686–3698. [PubMed: 25143397]

26. Silflow CD, and Lefebvre PA (2001) Assembly and motility of eukaryotic cilia and flagella. Lessons from Chlamydomonas reinhardtii. Plant Physiol. 127, 1500–1507. [PubMed: 11743094]
27. Asleson CM, and Lefebvre PA (1998) Genetic analysis of flagellar length control in Chlamydomonas reinhardtii: a new long-flagella locus and extragenic suppressor mutations. Genetics. 148, 693–702. [PubMed: 9504917]
28. Barsel SE, Wexler DE, and Lefebvre PA (1988) Genetic analysis of long-flagella mutants of Chlamydomonas reinhardtii. Genetics. 118, 637–648. [PubMed: 3366366]
29. McVittie A (1972) Flagellum mutants of Chlamydomonas reinhardii. J Gen Microbiol. 71, 525–540. [PubMed: 4647471]
30. Ishikawa H, Ide T, Yagi T, Jiang X, Hirono M, Sasaki H, Yanagisawa H, Wemmer KA, Stainier DY, Qin H, Kamiya R, and Marshall WF (2014) TTC26/DYF13 is an intraflagellar transport protein required for transport of motility-related proteins into flagella. Elife. 3, e01566. [PubMed: 24596149]
31. Kuchka MR, and Jarvik JW (1987) Short-Flagella Mutants of Chlamydomonas reinhardtii. Genetics. 115, 685–691. [PubMed: 17246376]
32. Nakamura S, Takino H, and Kojima MK (1978) Effect of lithium on flagellar length in Chlamydomonas reinhardtii. Cell Struct. Funct 12, 369–374.
33. Avasthi P, Marley A, Lin H, Gregori-Puigjane E, Shoichet BK, von Zastrow M, and Marshall WF (2012) A chemical screen identifies class a g-protein coupled receptors as regulators of cilia. ACS Chem Biol. 7, 911–919. [PubMed: 22375814]
34. Engel BD, Ishikawa H, Feldman JL, Wilson CW, Chuang PT, Snedecor J, Williams J, Sun Z, and Marshall WF (2011) A cell-based screen for inhibitors of flagella-driven motility in Chlamydomonas reveals a novel modulator of ciliary length and retrograde actin flow. Cytoskeleton. 68, 188–203. [PubMed: 21360831]
35. Witman GB, Rosenbaum JL, Berliner J, and Carlson K (1972) Chlamydomonas Flagella .1. Isolation and Electrophoretic Analysis of Microtubules, Matrix, Membranes, and Mastigonemes. Journal of Cell Biology. 54, 507. [PubMed: 4558009]
36. Pazour GJ, Agrin N, Leszyk J, and Witman GB (2005) Proteomic analysis of a eukaryotic cilium. Journal of Cell Biology. 170, 103–113. [PubMed: 15998802]
37. Rosenbaum JL, Moulder JE, and Ringo DL (1969) Flagellar elongation and shortening in Chlamydomonas. The use of cycloheximide and colchicine to study the synthesis and assembly of flagellar proteins. J Cell Biol. 41, 600–619. [PubMed: 5783876]
38. Cole DG, Diener DR, Himelblau AL, Beech PL, Fuster JC, and Rosenbaum JL (1998) Chlamydomonas kinesin-II-dependent intraflagellar transport (IFT): IFT particles contain proteins required for ciliary assembly in Caenorhabditis elegans sensory neurons. J Cell Biol. 141, 993–1008. [PubMed: 9585417]
39. Curry AM, and Rosenbaum JL (1993) Flagellar radial spoke: a model molecular genetic system for studying organelle assembly. Cell Motil Cytoskeleton. 24, 224–232. [PubMed: 8477455]
40. Yang P, Diener DR, Yang C, Kohno T, Pazour GJ, Dienes JM, Agrin NS, King SM, Sale WS, Kamiya R, Rosenbaum JL, and Witman GB (2006) Radial spoke proteins of Chlamydomonas flagella. J Cell Sci. 119, 1165–1174. [PubMed: 16507594]
41. Luck D, Piperno G, Ramanis Z, and Huang B (1977) Flagellar mutants of Chlamydomonas: studies of radial spoke-defective strains by dikaryon and revertant analysis. Proc Natl Acad Sci USA. 74, 3456–3460. [PubMed: 269405]
42. Khalifa AAZ, Ichikawa M, Dai D, Kubo S, Black CS, Peri K, McAlear TS, Veyron S, Yang SK, Vargas J, Bechstedt S, Trempe JF, and Bui KH (2020) The inner junction complex of the cilia is an interaction hub that involves tubulin post-translational modifications. Elife. 9, e52760 [PubMed: 31951202]
43. Yanagisawa HA, Mathis G, Oda T, Hirono M, Richey EA, Ishikawa H, Marshall WF, Kikkawa M, and Qin H (2014) FAP20 is an inner junction protein of doublet microtubules essential for both the planar asymmetrical waveform and stability of flagella in Chlamydomonas. Mol Biol Cell. 25, 1472–1483. [PubMed: 24574454]

44. Follit JA, Tuft RA, Fogarty KE, and Pazour GJ (2006) The intraflagellar transport protein IFT20 is associated with the Golgi complex and is required for cilia assembly. Mol Biol Cell. 17, 3781–3792. [PubMed: 16775004]
45. Diener DR, Ang LH, and Rosenbaum JL (1993) Assembly of flagellar radial spoke proteins in Chlamydomonas: identification of the axoneme binding domain of radial spoke protein 3. J Cell Biol. 123, 183–190. [PubMed: 8408197]
46. Ludington WB, Ishikawa H, Serebrenik YV, Ritter A, Hernandez-Lopez RA, Gunzenhauser J, Kannegaard E, and Marshall WF (2015) A systematic comparison of mathematical models for inherent measurement of ciliary length: how a cell can measure length and volume. Biophys J 108, 1361–1379 [PubMed: 25809250]
47. Quarmby LM, and Hartzell HC (1994) Two distinct, calcium-mediated, signal transduction pathways can trigger deflagellation in Chlamydomonas reinhardtii. J Cell Biol. 124, 807–815. [PubMed: 8120101]
48. Richey E, and Qin H (2013) Isolation of intraflagellar transport particle proteins from Chlamydomonas reinhardtii. Methods Enzymol. 524, 1–17. [PubMed: 23498731]
49. Osuna J, Perez-Blancas A, and Soberon X (2002) Improving a circularly permuted TEM-1 b-lactamase by directed evolution. Protein Eng. Design Sel 15, 463–470.
50. Minoura I, and Muto E (2006) Dielectric measurement of individual microtubules using the electroorientation method. Biophys. J 90, 3739–3748 [PubMed: 16500962]
51. Lin SP, Pan CY, Tseng KC, Lin MC, Chen CD, Tsai CC, Yu SH, Sun YC, Lin TW, and Chen YT (2009) A reversible surface functionalized nanowire transistor to study protein-protein interactions. Nano Today. 4, 235–243.
52. Zhang G, Johnston T, Quinn MB, and Schmidt-Dannert C (2019) Developing a protein scaffolding system for rapid enzyme immobilization and optimization of enzyme functions for biocatalysis. ACS Synth. Biol 8, 1867–1876. [PubMed: 31305981]
53. Lee MJ, Mantell J, Hodgson L, Alibhai D, Fletcher JM, Brown IR, Frank S, Xue W-F, Verkade P, Woolfson DN, and Warren MJ (2018) Engineered synthetic scaffolds for organizing proteins within the bacterial cytoplasm. Nat. Chem. Biol 14, 142–147. [PubMed: 29227472]
54. Nielsen AA, Der BS, Shin J, Vaidyanathan P, Paralanov V, Strychalski EA, Ross D, Densmore D, and Voigt CA (2016) Genetic circuit design automation. Science 352, aac7341 [PubMed: 27034378]
55. Dueber JE, Yeh BJ, Chak K, Lim WA (2003) Reprogramming control of an allosteric signalling switch through molecular recombination. Science 301, 1904–8. [PubMed: 14512628]
56. Toffoli T (1977) Computation and construction universality of reversible cellular automata. J. Comput. Syst. Sci 15, 213–231.
57. Csaba G, Porod W (2020) Coupled oscillators for computing: A review and perspective. Appl. Phys. Rev 7, 011302
58. Mallick A, Bashar MK, Truesdell DS, Calhoun BH, Joshi S, Shukla N (2020) Using synchronized oscillators to compute the maximum independent set. Nat. Comm 11, 4689
59. Harris EH, Stern DB, and Witman GB. eds. 2009. Chapter 8 - Chlamydomonas in the Laboratory. In The Chlamydomonas Sourcebook (Second Edition) (Academic Press, London), pp 241–302
60. Zhao L, Hou Y, Picariello T, Craige B, Witman GB (2019) Proteome of the central apparatus of a ciliary axoneme. J. Cell Biol 218, 2051–2076 [PubMed: 31092556]
61. Dai D, Ichikawa M, Peri K, Rebinsky R, and Bui KH (2020) Identification and mapping of central pair proteins by proteomic analysis. Biophys. Physicobiol 17, 71–85 [PubMed: 33178545]
62. Ma M, Stoyanova M, Rademacher G, Dutcher SK, Brown A, and Zhang R (2019) Structure of the decorated ciliary doublet microtubule. Cell 179, 909–922. [PubMed: 31668805]
63. Gui M, Ma M, Sze-Tu E, Wang X, Koh F, Zhong ED, Berger B, Davis JH, Dutcher SK, Zhang R, and Brown A (2021) Nat. Struct. Mol. Biol 28, 29–37. [PubMed: 33318703]
64. Weeks DP, and Collis PS (1976) Induction of microtubule protein synthesis in Chlamydomonas reinhardi during flagellar regeneration. Cell 8, 15–27.

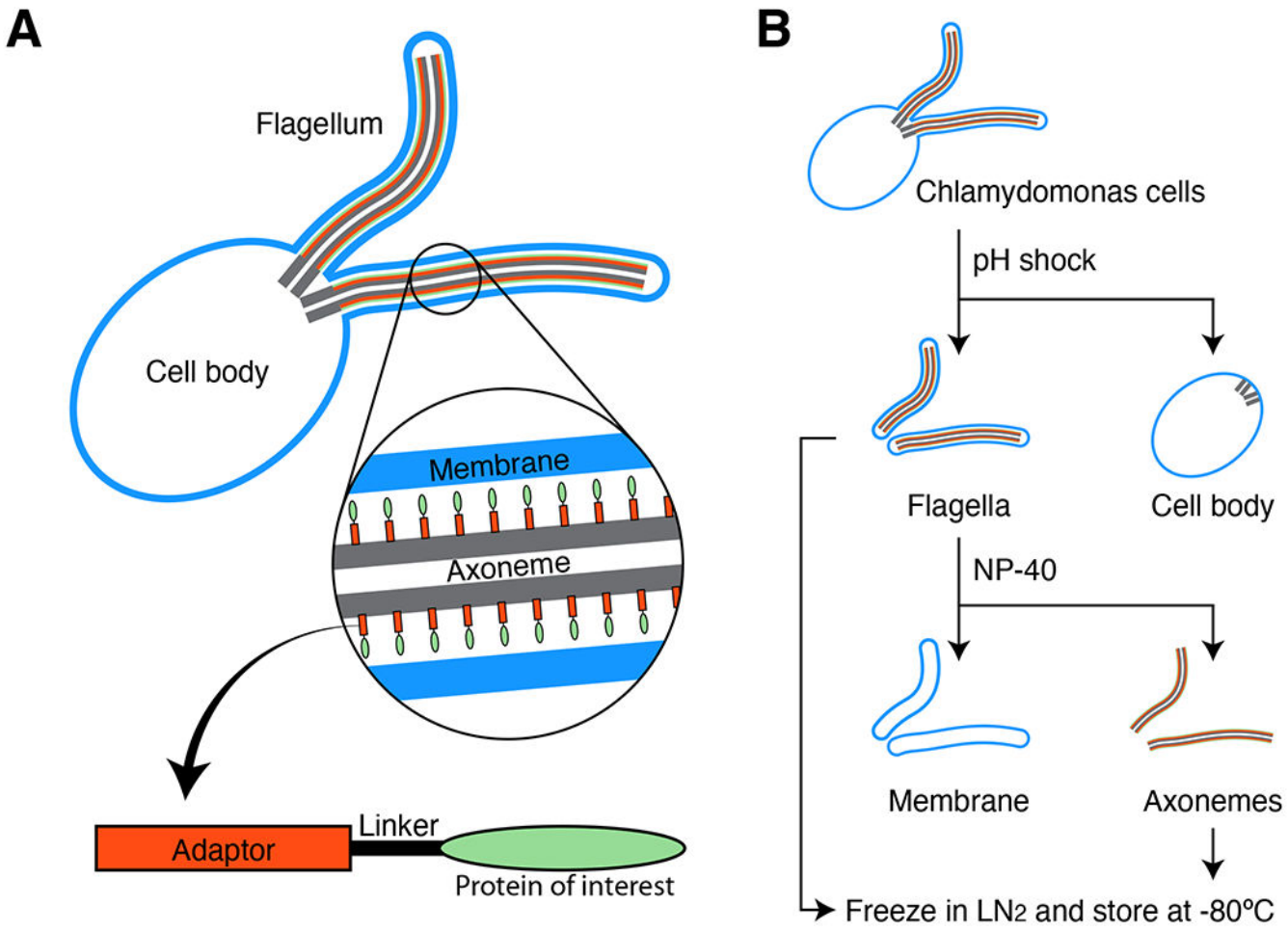


**Figure 1.**

Harnessing the flagellar axoneme as a biologically self-assembling protein nanoarray. (A) *Chlamydomonas* algal cells contain two flagella that protrude from the cell surface. The structural core of the flagellum is the axoneme, an array of nine doublet microtubules that is, in turn, surrounded by the flagellar membrane. By fusing a protein of interest to one of the axonemal proteins, the axoneme protein can serve as an adaptor to attach many copies of the protein of interest into the axoneme, forming a protein array. (B) One-step purification and low-cost harvesting of protein arrays in multiple forms. Flagella can be cleanly detached from the cell body by transiently reducing the pH of the media (pH shock), which releases the cell body intact, allowing the flagellum to be isolated in a single centrifugation or filtration step. The flagellum can be stored in this form, or can be treated with detergent to remove the membrane, producing a naked axoneme where the fusion proteins are directly exposed. This system therefore allows the protein array to be isolated in either a membrane-bound vesicle form or a solvent exposed membrane-less form.

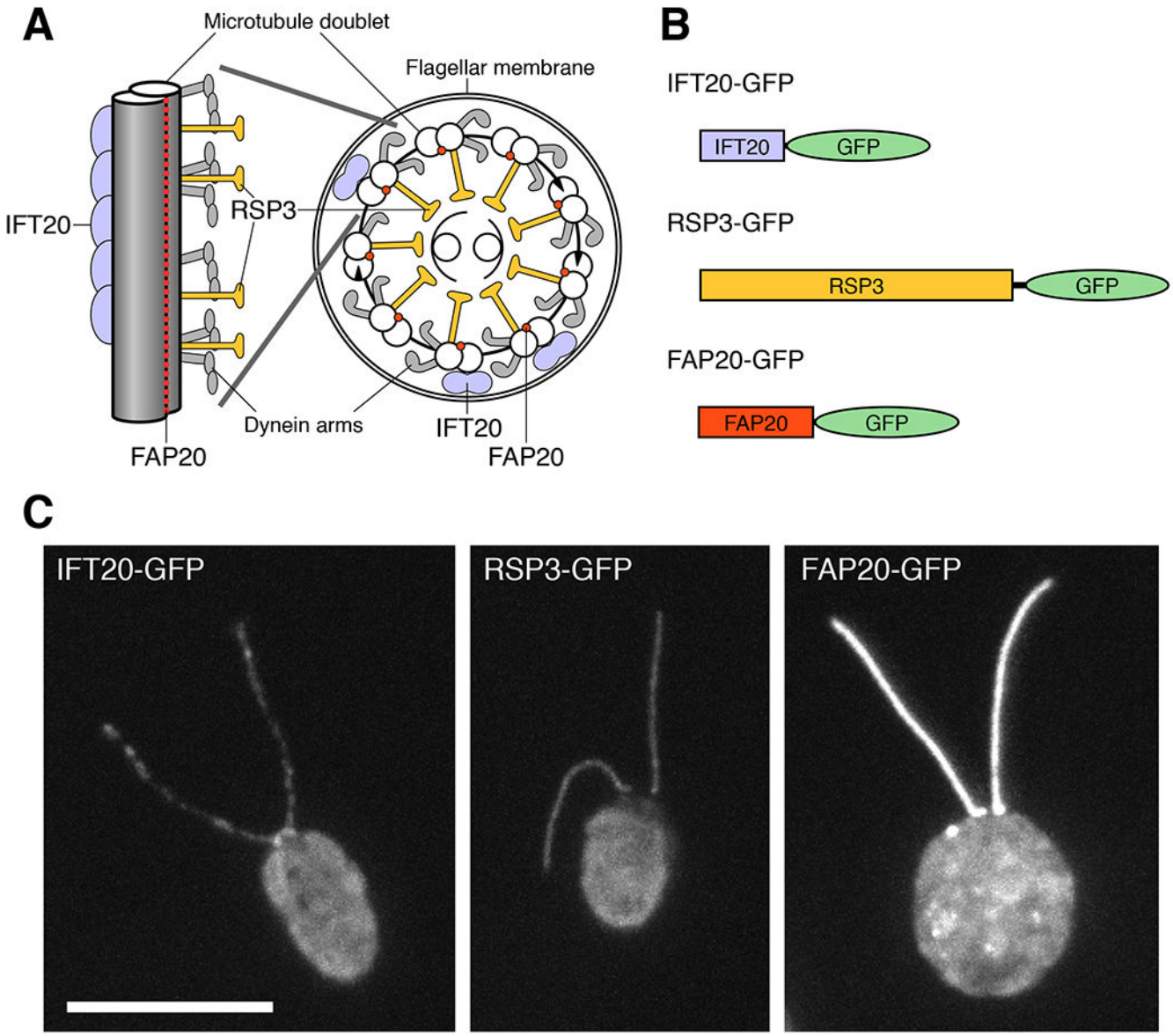


**Figure 2.**

Adaptor proteins for axonemal nanoarray. (A) Cross section and longitudinal views of axoneme showing location of IFT20, RSP3, and FAP20 in their respective complexes. RS, radial spoke; IFT, intraflagellar transport. (B) Diagram of constructs showing where GFP is fused to the protein. (C) *Chlamydomonas* cells expressing GFP-tagged fusion constructs with IFT20, RSP3, and FAP20. Scale bar, 10 μm.

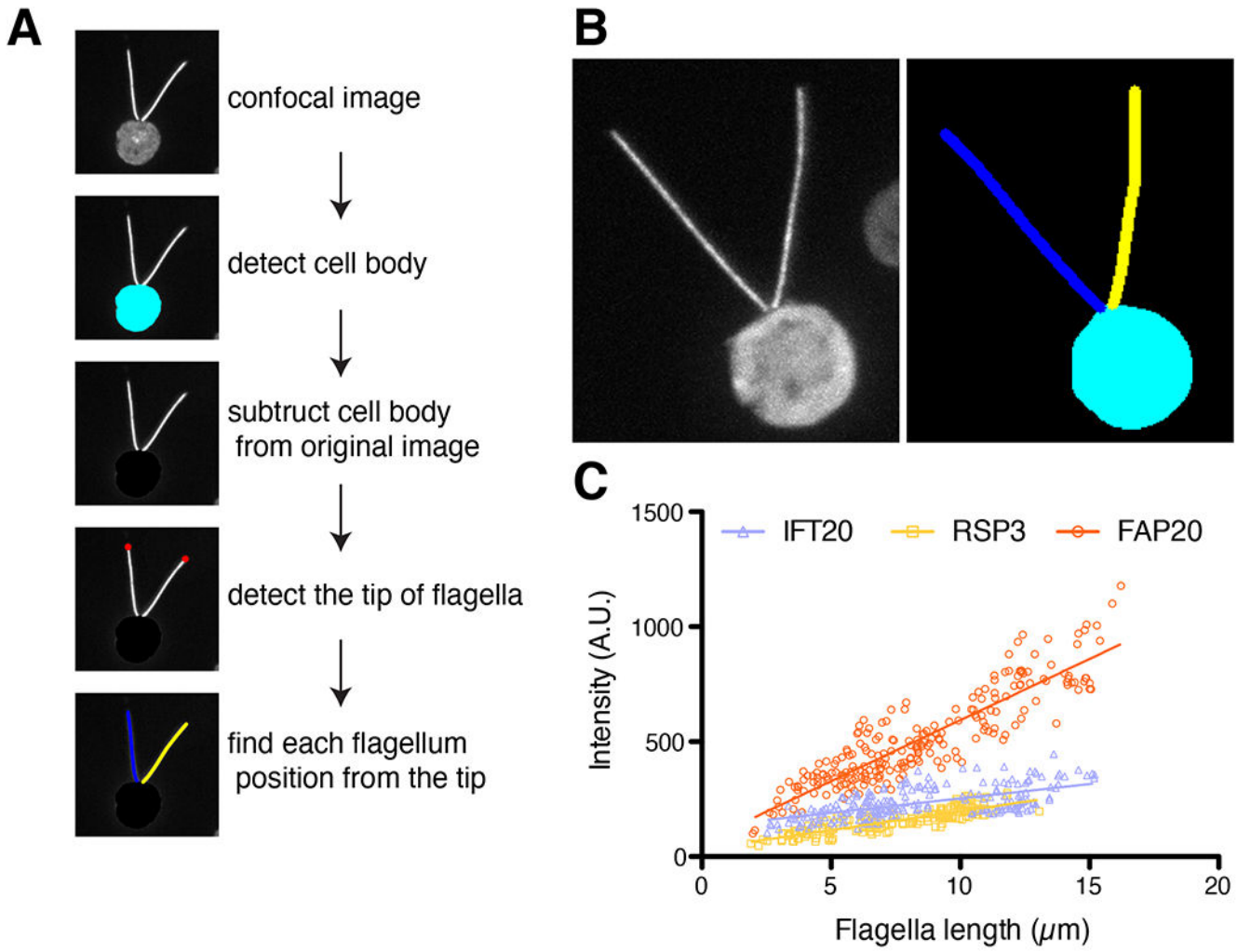


**Figure 3.**

Quantification of GFP incorporation into flagella. (A) Diagram to show the steps of the image analysis algorithm. (B) illustrative example showing segmentation of the flagella. (C) Graph of total GFP intensity versus flagellar length for the three constructs.

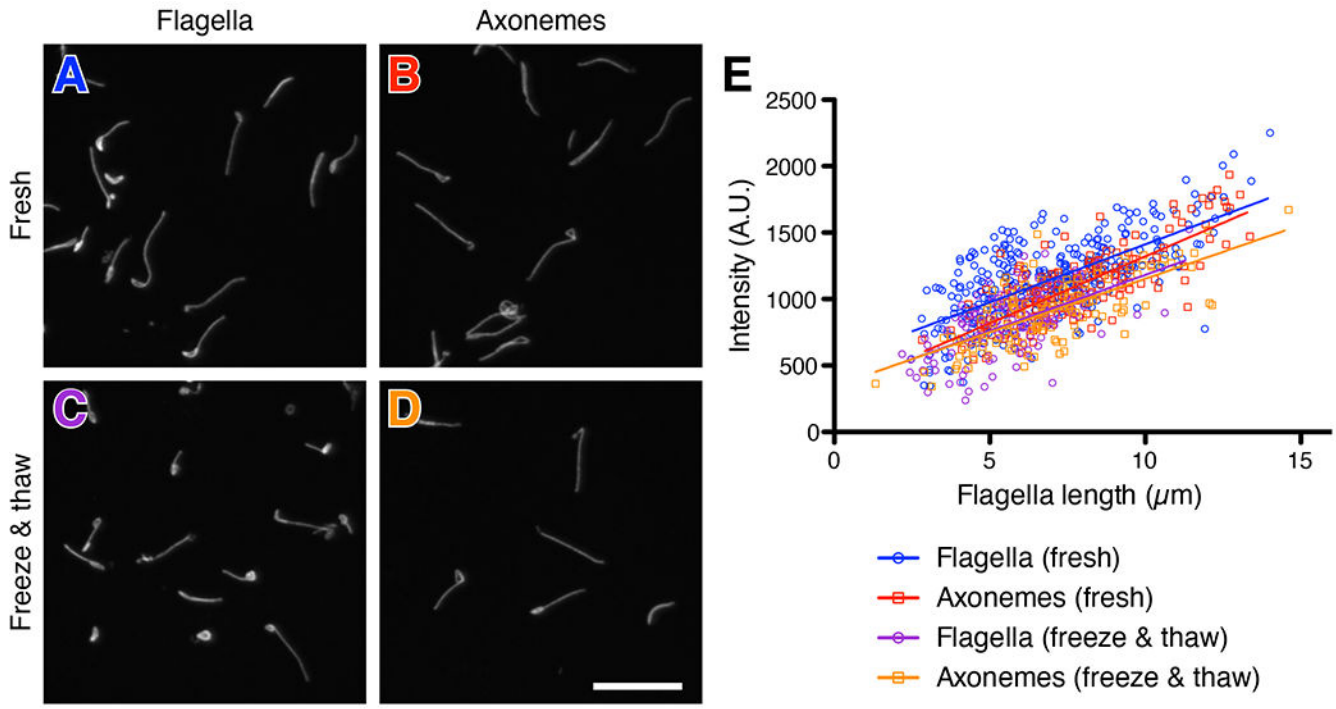


**Figure 4.**

Stability of FAP20-GFP during nanoarray isolation and storage. (A,B) Images of detached flagella following pH shock before (A) and after (B) demembranation to produce axonemes. (C,D) Detached flagella (C) and axonemes (D) following storage at −80°C. Scale bar for (A-D) 10 μm. (E) Quantification of GFP fluorescence showing retention of signal during axoneme preparation. Freeze-thaw does result in a small decrease in signal.

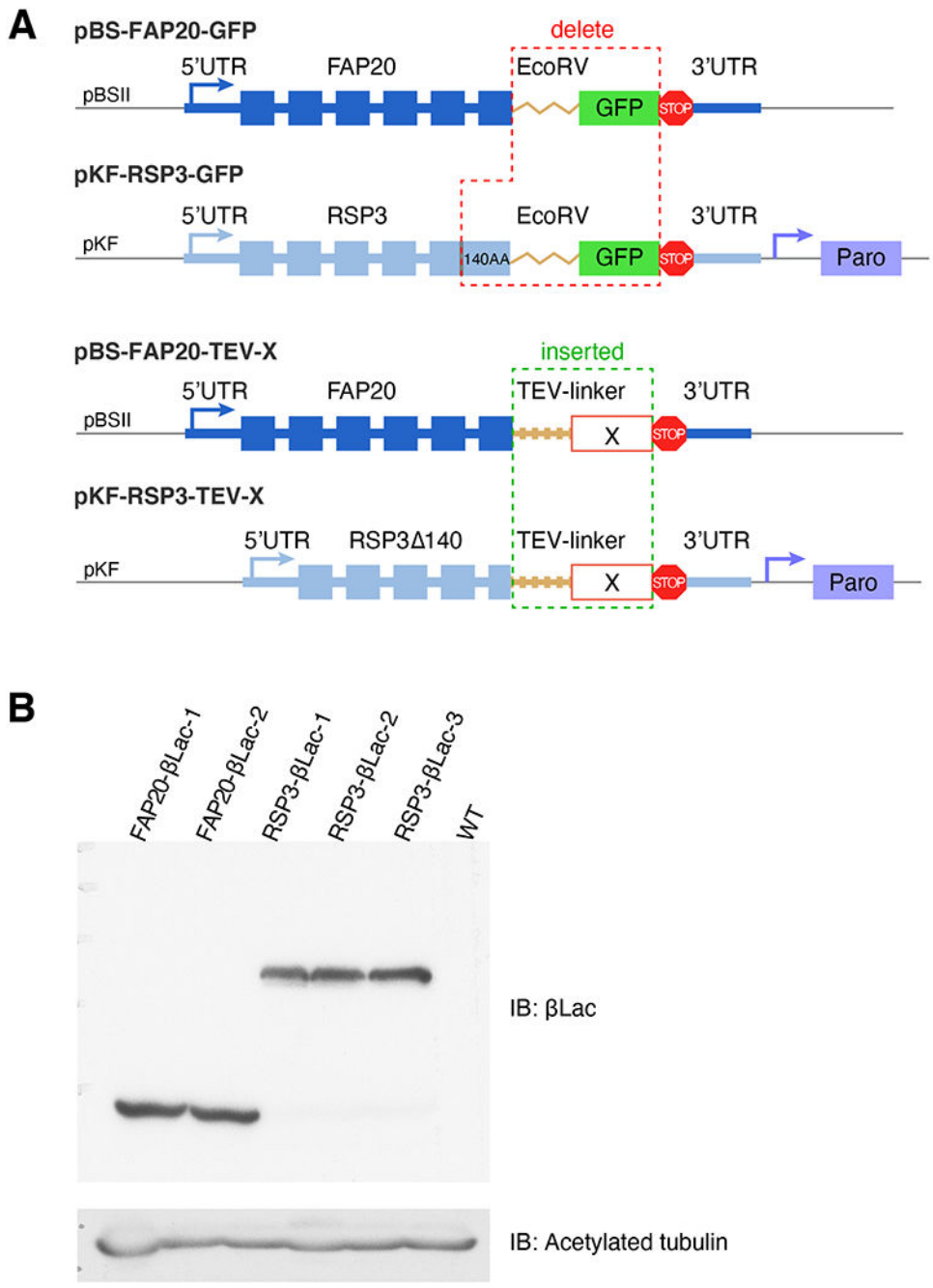


**Figure 5.**

Constructs for expressing fusion proteins. (A) The constructs of pBS-FAP20-GFP and pKF-RSP3-GFP [43] were modified to express the fusion proteins. The fusion protein was connected to FAP20 or RSP3 with a TEV-linker. The restriction enzyme EcoRV digestion sequence and the GFP gene were deleted in both of the original constructs. In addition, the C-terminal 140 amino acids of RSP3 were deleted as well in the pKF-RSP3-GFP construct. The TEV-linker and the target gene (X), such as βLac, were fused to the C-terminus of either FAP20 or RSP3. (B) The concentration of flagella samples was adjusted to

1.6 μg/μL with the dilution of HMDEK buffer and subjected to Western blotting. The immunoblotting of βLac showed the protein expression levels in each of the flagella samples and immunoblotting of acetylated tubulin showed the equal loading of each sample.

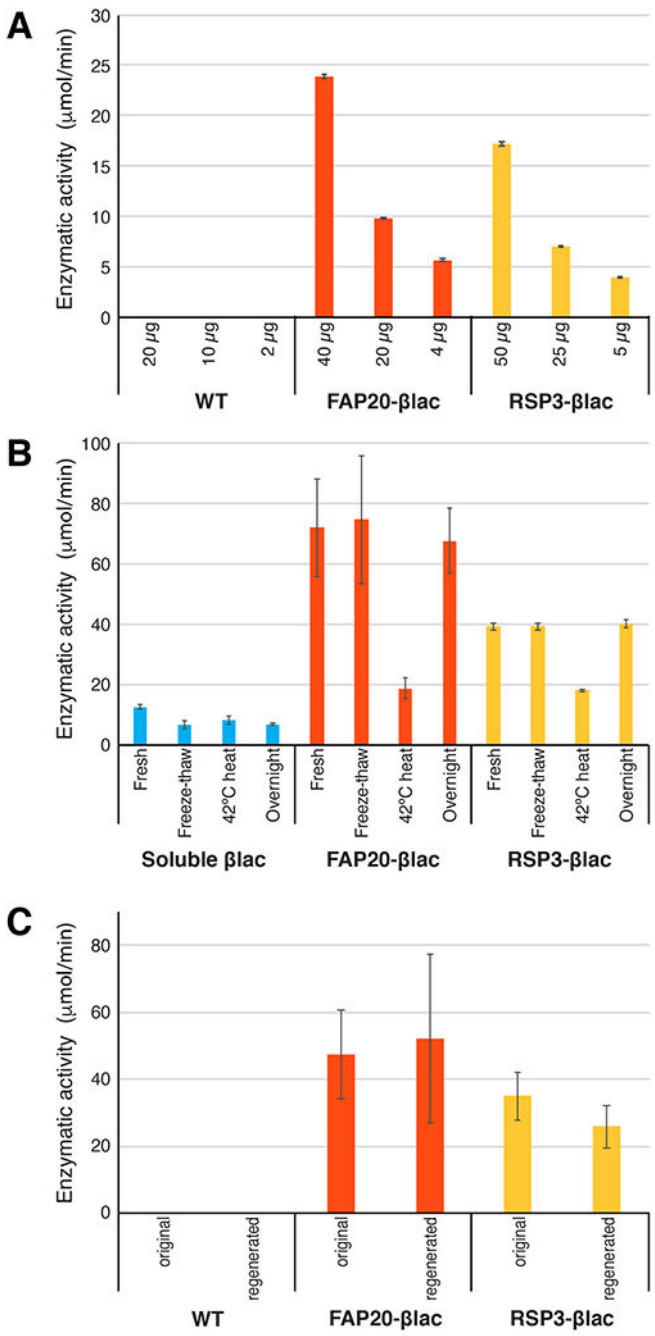


**Figure 6.**

Axoneme-based enzyme arrays using βLac. (A) βLac activity is undetectable in WT *Chlamydomonas* flagella but is conferred by flagella containing FAP20 or RSP3 βLac fusion constructs. Protein quantity listed is the total quantity of isolated flagella added to the assay. (B) βLac activity in axonemes compared with soluble enzyme. For the soluble enzyme, 2.5 μg of lyophilized protein was resuspended and used in the assay, while for axonemes, 8 μg of total axonemal protein was used. (C) Recovery of enzyme activity in recycled flagella.

The flagella from the first reaction were collected and re-subjected to a new reaction. Two replicates were performed for the enzymatic activity assay.

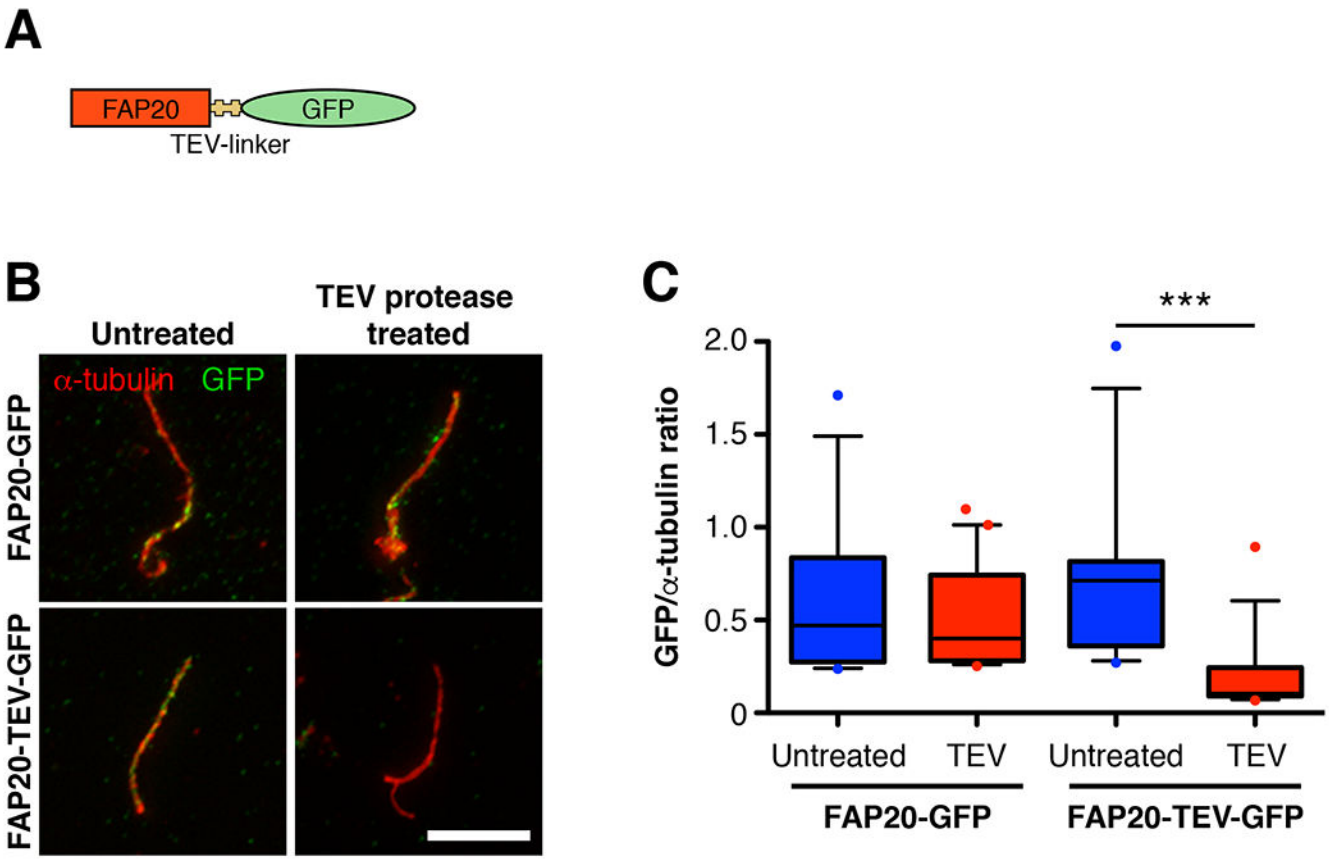


**Figure 7.**

Release of fusion constructs by TEV protease treatment. (A) Diagram of modified construct that includes a TEV protease cleavage site. (B) Comparing untreated versus TEV protease treated axonemes from FAP20-GFP and FAP20-TEV-GFP strains. Isolated axonemes were fixed and stained with antibodies to alpha tubulin (red) and GFP (green) after treatment with TEV protease. Note that the granular appearance of the GFP signal compared to earlier images is an artifact of methanol fixation required to image the alpha-tubulin staining. Reduced green fluorescence in axonemes treated with TEV protease demonstrates release of most of the GFP domain from the fusion construct. Scale bar, 5 μm. (C) Quantification of GFP release by TEV protease cleavage. Box plot shows the ratio of GFP/alpha-tubulin fluorescent intensity for untreated and TEV protease treated axonemes of FAP20-GFP and FAP20-TEV-GFP (n=18,19,13, and 18, respectively). Two-sided Student's t-test *** $P < 0.001$.